

# An Accurate Frequency-Dependent Analytical Expression for Leakage Inductance Calculation in High Frequency Transformers

M. A. Bahmani, Student Member, IEEE, T. Thiringer, Member, IEEE

## Abstract

Pushing magnetic components towards higher power densities, which is often realized by increasing the operating frequency, leads to the need for the development of more accurate design tools, for example more accurate expressions for core losses, winding losses and leakage inductance calculations. This paper presents a new analytical expression intended to accurately evaluate the leakage inductance of transformers in the high frequency range in which the behavior of the magnetic field within the windings is altered. Unlike conventional expressions, which usually overestimate the leakage inductance at higher frequencies, this expression accounts for high frequency behavior of the magnetic field and provides high accuracy when operating at high frequencies. These high accuracy and applicability makes the derived expression of interest for designers to avoid time consuming finite element simulations without compromising with accuracy. The expression is validated by 2-D FEM simulation, as well as by measurements.

## I. INTRODUCTION

High power densities in power conversion units have become one of the design requirements, particularly in high restriction applications such as traction and offshore wind farms [1], [2]. To achieve this goal, the bulky 50/60 Hz transformers have been replaced with high power density DC-DC converters consisting of high-frequency transformers with lower weights and volumes. However, being exposed to higher frequencies, one should cope with extra losses coming from eddy current losses in the magnetic core [3], [4], excess losses in the windings due to enhanced skin and proximity effects [5], as well as parasitic elements, i.e., leakage inductance [6]–[8] and winding capacitance [9], [10], causing excess switching losses in the power semiconductors which is usually dominant at higher frequencies [11].

Recently, there has been growing interest in utilizing dual active bridge (DAB) converters in high power applications [12]. The equivalent circuit of a DAB converter is shown in Fig. 1 in which two square voltage waveforms on two sides of the transformer have been shifted by controlling the input and output bridges. This applies full voltage on the inductance,  $L$ , which is used to shape the current as a power transfer element [13]. In order to achieve zero voltage switching (ZVS), the phase shift between the bridges,  $\varphi$ , should be higher than a certain value resulting in the series inductance minimum value as presented in (1). This inductance, as shown in Fig. 1, is often integrated in the high frequency transformer as the leakage inductance,  $L_\sigma$ , in order to reduce the number of components, hence achieving higher power densities.

$$L = \frac{V_{DC1}V_{DC2}\varphi \cdot (\pi - \varphi)}{2P_{out}\pi^2 f_s n} \quad (1)$$

Moreover, in some applications such as resonant converters the value of  $L_\sigma$  should be tuned in order to incorporate the leakage inductance as one of the resonant elements to retain the resonant conditions [14], [15]. Hence, accurate evaluation of leakage inductance in the design process is of great importance for designers, more specifically in high power density applications where high deviations between the calculated and actual value can not be easily tolerated.

The purpose of this paper is to propose a new analytical model to calculate a fairly precise value of leakage inductance. This model takes into account the effects of high frequency fields inside the conductors with all the geometrical parameters of the transformer windings when determining the leakage inductance. Being validated by FEM simulations and measurements on different winding configurations, this model provides a very good accuracy with wide-range applicability which could be of interest for designers to avoid time consuming FEM simulation without compromising with the accuracy.

Section II of this paper explains the methodology used to derive the final frequency-dependent formula. Section III provides a wide range comparison between classical methods and the new frequency-dependent expression in terms of accuracy and domain of validity. In Section IV, the experimental results are presented and finally, Section V provides the conclusions.

Copyright (c) 2014 IEEE. Personal use of this material is permitted. However, permission to use this material for any other purposes must be obtained from the IEEE by sending a request to pubs-permissions@ieee.org.

The project is financially supported by the Swedish Energy Agency.

M. Amin Bahmani and Torbjörn Thiringer are with Chalmers University of Technology, SE-412 96 Gothenburg, Sweden (e-mail: bahmani@chalmers.se; torbjorn.thiringer@chalmers.se;).

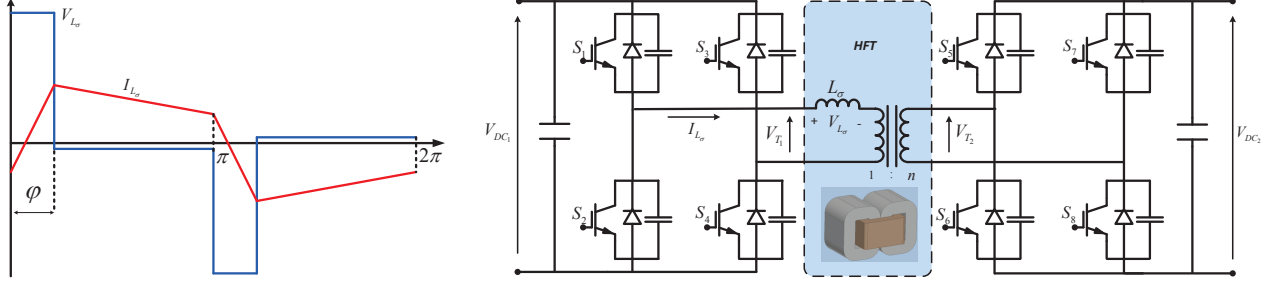


Fig. 1: Equivalent circuit of a dual active bridge converter along with the leakage inductance integrated in to the high frequency transformer, as well as the voltage and current of the leakage inductance

## II. EXPRESSION DERIVATION

Fig. 2 shows a sample 2D axisymmetric FEM simulation of the transformer windings at different values of penetration ratio,  $\Delta$  as defined in (11), illustrating the computed current density distribution and magnetic field intensity in the primary and secondary windings respectively. The dimensions of the geometry were kept constant and different values of  $\Delta$  were achieved by applying the frequencies corresponding to those values. In other words, the analysis is based on a dimensionless parameter,  $\Delta$ , taking into account the effects of both frequency and geometrical dimensions. The normalised magnetic field intensity distribution on inter and intra-layer spaces, obtained from the same FEM simulation at four different values of  $\Delta$ , are shown in Fig. 2 bottom.

$$\begin{aligned}
 W_{leakage} &= \frac{1}{2} \mu \int H^2 dv \\
 &= \frac{1}{4} L_{\sigma(pri)} I_1^2 \\
 &= W_{pri} + W_{ins(1)} + W_{isolation} + W_{sec} + W_{ins(2)}
 \end{aligned} \tag{2}$$

As can be seen in Fig. 2, the magnetic field intensity inside the copper windings drastically decreases by increasing the frequency or its corresponding  $\Delta$ . Thus results in lower value of leakage inductances since the leakage inductance is strongly correlated to the magnetic field intensity, as in (2), within the transformer window. This causes higher ohmic losses on the third layer of the primary windings than the ohmic losses in the first and second layer. This is because of the fact that in contrast to the first layer, which does not suffer from the magnetic field on its left hand side, the second layer and more significantly the third layer suffers from the presence of the magnetic field on their left hand side. This magnetic field drop at higher frequency is often neglected in most of the classical formulas for leakage inductance calculations which might result to inaccuracy in high power density applications.

Fig. 3 shows the schematic of a transformer window comprising the magnetic core with a relatively high permeability of 20000, copper foil primary windings consisting of  $m_1$  layers and  $N_{l1}$  turns per layer, secondary round magnet wires consisting of  $m_2$  layers and  $N_{l2}$  turns per layer and all the corresponding distances, i.e. isolation distance, insulating distance, winding heights and thicknesses and so on.

As shown in (2), the energy stored in the magnetic field of a transformer when the secondary windings is shorted is equal to the energy stored in the leakage inductance referred to the primary side of the transformer. Therefore, one can separately derive the stored energy within isolation distance, primary and secondary inter-layer insulations and primary and secondary copper areas, respectively. First, the energy stored within isolation and insulation distances are calculated since the magnetic field intensity within these regions are constant, hence using (2) and considering a one dimensional magnetic field, one can conclude:

$$\begin{aligned}
 W_{isolation} &= \frac{1}{4} \mu M L T_{isolation} h_w \int_0^{d_{iso}} \left( \frac{N_{l1} m_1 I_1}{h_w} \right)^2 . dx \\
 &= \frac{1}{4} \mu M L T_{isolation} \frac{N_{l1}^2 m_1^2 I_1^2}{h_w} d_{iso}
 \end{aligned} \tag{3}$$

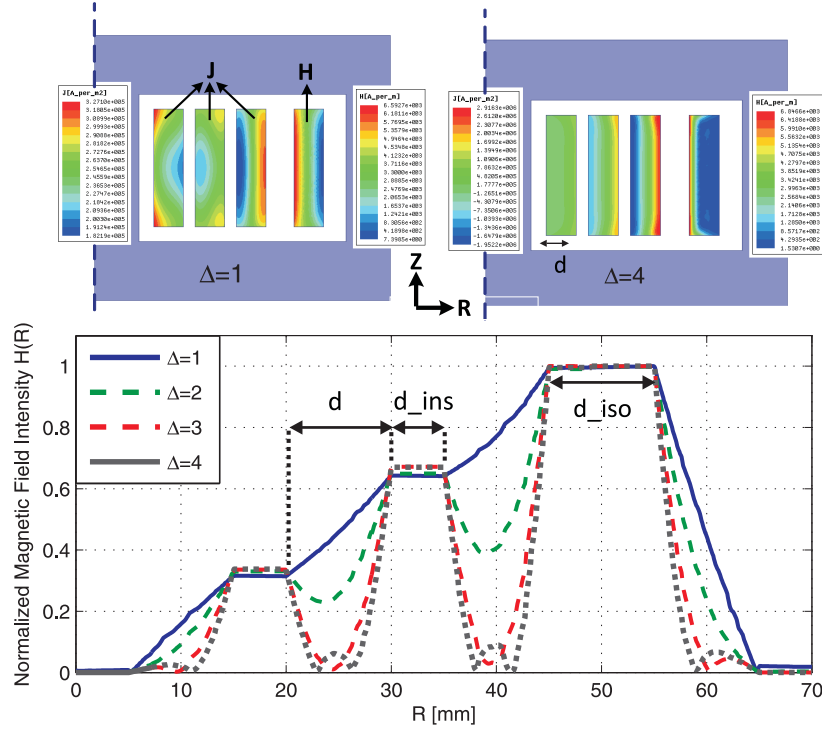


Fig. 2: The magnetic field distribution profile within the transformer window at different frequencies.

$$\begin{aligned}
 W_{ins1} &= \frac{1}{4} \mu M L T_{pri} h_w \left[ \sum_{n=0}^{m_1-1} \frac{N_{l1}^2 n^2 I_1^2}{h_w^2} d_{ins1} \right] \\
 &= \frac{1}{4} \mu M L T_{pri} \frac{N_{l1}^2}{h_w} I_1^2 d_{ins1} \frac{m_1(m_1-1)(2m_1-1)}{6}
 \end{aligned} \tag{4}$$

$$\begin{aligned}
 W_{ins2} &= \frac{1}{4} \mu M L T_{sec} h_w \left[ \sum_{n=0}^{m_2-1} \frac{N_{l2}^2 n^2 I_2^2}{h_w^2} d_{ins2} \right] \\
 &= \frac{1}{4} \mu M L T_{sec} \frac{N_{l1}^2}{h_w} I_1^2 d_{ins2} \frac{m_2^2(m_2-1)(2m_2-1)}{6m_2}
 \end{aligned} \tag{5}$$

where  $M L T_{pri}$ ,  $M L T_{sec}$  and  $M L T_{iso}$  are the mean length turns of the primary portion, secondary portion and isolation distance, respectively.  $h_w$  is the winding height,  $I_1$  and  $I_2$  are the peak current values of primary and secondary portions, respectively.

However, obtaining a closed formula for the stored energy inside the copper windings is not as straightforward as what were obtained in (3) to (5) since the magnetic field pattern is not constant or linear at higher frequencies as already shown in Fig. 2. In fact, the magnetic field has a hyperbolic pattern according to Dowell's derivation [16]. Substituting this hyperbolic pattern in (2), one can derive:

$$\begin{aligned}
 W_{pri} &= \frac{1}{4} \mu M L T_{pri} h_w \sum_{n=1}^{m_1} \left( \int_0^{d_{pri}} H_x^2 dx \right) \\
 &= \frac{1}{4} \mu M L T_{pri} h_w \sum_{n=1}^{m_1} \left( \int_0^{d_{pri}} \left[ \frac{H_{ex} \sinh(\alpha x) - H_{in} \sinh(\alpha x - \alpha d_{pri})}{\sinh(\alpha d_{pri})} \right]^2 dx \right)
 \end{aligned} \tag{6}$$

$$\begin{aligned}
 W_{sec} &= \frac{1}{4} \mu M L T_{sec} h_w \sum_{n=1}^{m_2} \left( \int_0^{d_{sec}} H_x^2 dx \right) \\
 &= \frac{1}{4} \mu M L T_{sec} h_w \sum_{n=1}^{m_2} \left( \int_0^{d_{sec}} \left[ \frac{H_{ex} \sinh(\alpha x) - H_{in} \sinh(\alpha x - \alpha d_{sec})}{\sinh(\alpha d_{sec})} \right]^2 dx \right)
 \end{aligned} \tag{7}$$

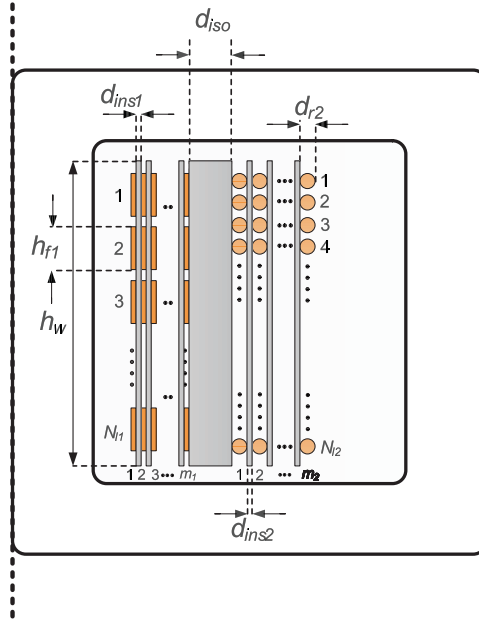


Fig. 3: Cross-sectional view of the winding configurations according to Dowell's assumptions.

where  $H_{in}$  and  $H_{ex}$  are the magnetic field intensity at the left and right hand side of each winding layer and can be calculated as (8). Also,  $\alpha$  is defined as  $\frac{1+j}{\delta}$  where  $\delta$  is the skin depth at any particular frequency and  $d_{pri}$  and  $d_{sec}$  are the thickness of the primary and secondary conductors, respectively,

$$H_{in} = \frac{(n-1)N_{l1}I_1}{h_w} \quad H_{ex} = \frac{nN_{l1}I_1}{h_w} \quad (8)$$

Substitution of (8) into (6) and (7) and rearranging for the stored energy gives

$$W_{pri} = \frac{1}{4}\mu M L T_{pri} \frac{N_{L1}^2}{h_w} m_1 I_1^2 \left[ \frac{\sin(\frac{2\Delta_1}{\alpha\delta})4\alpha\delta^2(m_1^2-1) + 4d_{pri}(2m_1^2+1) - \alpha\delta^2\sin(\frac{4\Delta_1}{\alpha\delta})(2m_1^2+1) + 8d_{pri}(1-m_1^2)\cos(\frac{2\Delta_1}{\alpha\delta})}{24\sin^2(\frac{2\Delta_1}{\alpha\delta})} \right] \quad (9)$$

$$W_{sec} = \frac{1}{4}\mu M L T_{sec} \frac{N_{L1}^2}{h_w} \frac{m_1^2}{m_2} I_1^2 \left[ \frac{\sin(\frac{2\Delta_2}{\alpha\delta})4\alpha\delta^2(m_2^2-1) + 4d_{sec}(2m_2^2+1) - \alpha\delta^2\sin(\frac{4\Delta_2}{\alpha\delta})(2m_2^2+1) + 8d_{sec} \cdot (1-m_2^2)\cos(\frac{2\Delta_2}{\alpha\delta})}{24\sin^2(\frac{2\Delta_2}{\alpha\delta})} \right] \quad (10)$$

where  $\Delta_1$  and  $\Delta_2$  are the penetration ratio of the primary and secondary winding as (11)

$$\Delta_1 = \frac{d_{pri}}{\delta} \quad \Delta_2 = \frac{d_{sec}}{\delta} \quad (11)$$

Finally, substitution of (3), (4), (5), (9) and (10) into (2) and rearranging for  $L_{\sigma(pri)}$  gives the final frequency-dependent expression as

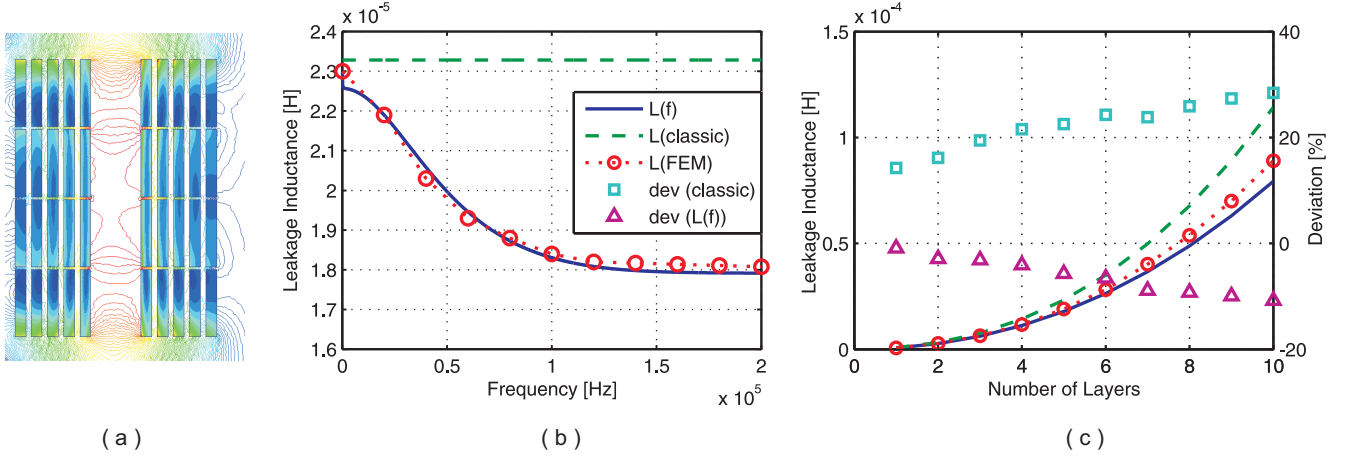


Fig. 4: (a) A sample FEM simulation result. (b) Calculated Leakage inductance by the studied methods versus frequency. (c) Calculated Leakage inductance by the studied methods versus the number of layers in each windings portion while the frequency is constant.

$$\begin{aligned}
L_{\sigma(\text{pri})} = & \mu \frac{N_1^2}{h_w} m_1 \left[ M L T_{\text{iso}} m_1 d_{\text{iso}} \right. \\
& + M L T_{\text{pri}} \frac{(m_1 - 1) \cdot (2m_1 - 1)}{6} d_{\text{ins1}} \\
& + M L T_{\text{sec}} \frac{m_1 \cdot (m_2 - 1) \cdot (2m_2 - 1)}{6m_2} d_{\text{ins2}} \\
& + M L T_{\text{pri}} \frac{\sin(\frac{2\Delta_1}{\alpha\delta}) 4\alpha\delta^2 (m_1^2 - 1) + 4d_{\text{pri}}(2m_1^2 + 1)}{24\sin^2(\frac{2\Delta_1}{\alpha\delta})} \\
& + M L T_{\text{pri}} \frac{-\alpha\delta^2 \sin(\frac{4\Delta_1}{\alpha\delta}) (2m_1^2 + 1) + 8d_{\text{pri}}(1 - m_1^2) \cos(\frac{2\Delta_1}{\alpha\delta})}{24\sin^2(\frac{2\Delta_1}{\alpha\delta})} \\
& + M L T_{\text{sec}} \frac{m_1 \sin(\frac{2\Delta_2}{\alpha\delta}) 4\alpha\delta^2 (m_2^2 - 1) + 4d_{\text{sec}}(2m_2^2 + 1)}{m_2 \cdot 24\sin^2(\frac{2\Delta_2}{\alpha\delta})} \\
& \left. + M L T_{\text{sec}} \frac{m_1 - \alpha\delta^2 \sin(\frac{4\Delta_2}{\alpha\delta}) (2m_2^2 + 1) + 8d_{\text{sec}}(1 - m_2^2) \cos(\frac{2\Delta_2}{\alpha\delta})}{m_2 \cdot 24\sin^2(\frac{2\Delta_2}{\alpha\delta})} \right] \quad (12)
\end{aligned}$$

It should be noted that the final expression has been derived based on foil winding configuration, however, it would be applicable for round conductors by modifying  $\Delta$  of the windings portion with round wire as

$$\Delta = \frac{d_r \sqrt{2}}{2\delta} \sqrt{\frac{N_l d_r \sqrt{\pi}}{2h_w}} \quad (13)$$

### III. ACCURACY INVESTIGATION

In order to investigate the accuracy of the aforementioned expression, parametric FEM simulations covering a wide range of frequency, up to 200 kHz, have been performed. The obtained leakage inductances were then compared with the leakage inductances calculated by the classical expressions [17], [18]. The investigated winding arrangement, illustrated in Fig. 4(a), consists of 20 foil conductors in each winding portion, 5 layers and 4 turns per layer, with the foil thickness of 1.2 mm. All the geometrical dimensions are kept constant while the operating frequency is swept from 50 Hz to 200 kHz.

$$L_{\sigma(\text{classic})} = \mu M L T_{\text{pri}} \cdot \frac{m_1^2 \cdot N_{l1}^2}{h_w} \left( d_{\text{iso}} + \frac{m_1 \cdot d_{\text{pri}} + (m_1 - 1)d_{\text{ins1}} + m_2 \cdot d_{\text{sec}} + (m_2 - 1)d_{\text{ins2}}}{3} \right) \quad (14)$$

As can be seen in Fig. 4(b), the classical expression, (14), generally shows a high inaccuracy for almost the whole range of investigation, particularly at higher frequencies. For instance, at 200 kHz, the classical expression estimates the leakage inductance as high as 0.23  $\mu\text{H}$  whereas FEM simulation and the derived frequency-dependent expression shows 0.182  $\mu\text{H}$  and 0.18  $\mu\text{H}$  respectively. This significant overestimation can result in an unrealistic and costly magnetic design. This inaccuracy could stem from the rigorous assumption made regarding the linear pattern of the magnetic field within copper conductors

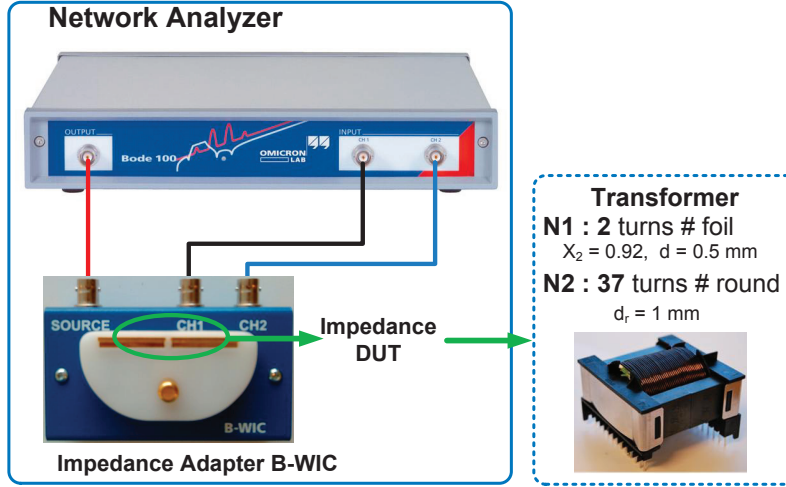


Fig. 5: Measurement setup and the manufactured transformer.

which is not a valid assumption when a conductor, conducting high frequency currents, is surrounded by a large number of other conductors with a complex arrangement. In fact, by increasing the frequency, the magnetic field inside the copper conductors falls quicker towards zero, consequently the leakage inductance decreases as can be seen in Fig. 4(b) where results are determined by FEM and the frequency-dependent formula. Exceeding a certain frequency, depending on geometrical characteristics of the windings, there would be almost no magnetic field within a conductor and thus no further decrease in the obtained leakage inductance. This attribute can be seen in Fig. 4(b) when the frequency exceeds  $120$  kHz.

Fig. 4(c) shows the obtained values of leakage inductance at different number of primary and secondary winding layers whereas the frequency is kept constant at  $150$  kHz. Moreover the deviation of the classical and frequency-dependent expressions from the results obtained by FEM have been calculated by

$$L_{\sigma(\text{deviation})}[\%] = 100 \times \frac{L_{\sigma(\text{calculated})} - L_{\sigma(\text{FEM})}}{L_{\sigma(\text{FEM})}} \quad (15)$$

As can be seen in Fig. 4(b) and (c), using the frequency-dependent formula, almost in the whole range of frequency and at different number of winding layers, the leakage inductance were calculated with a negligible difference from the FEM results indicating the high accuracy of the proposed expression. In contrast, the classical formula generally shows a high inaccuracy for almost the whole range of frequency and different number of layers. According to the deviation curves illustrated in Fig. 4(c), classical expression leads to deviations of a 30% overestimation (with 10 layers of windings) whereas the frequency-dependent formula exhibit a deviation of always less than 10% underestimation, nevertheless at lower number of layers it is around 4%, within the studied range which is substantially more accurate than the classical expression. In addition,  $d_{ins2}$  and  $d_{iso}$  are about 1 and 2 mm, respectively.

#### IV. EXPERIMENTAL VALIDATION

In order to verify the accuracy of the proposed frequency dependent expression, a transformer comprising ETD59 Ferrite cores, two layers of foil conductors as the primary windings and one layer of solid round wire consisting of 37 turns as the secondary windings, has been manufactured. The thickness and diameter of the foil and round conductors are, respectively, 0.5 and 1 mm while the porosity factor, the degree of fulfillment of the core window height, is about 0.92. Using the network analyzer, Bode 100, the impedance of the transformer has been measured from the primary side while the secondary is shorted. The measurement setup and the manufactured transformer are shown in Fig. 5.

Fig. 6 demonstrates a comparison between the measured leakage inductance and the values calculated by the frequency dependent and classical expressions. The overall results indicate a good agreement between the frequency dependent expression and the measurements, whereas the classical expression is constant within the whole frequency range, demonstrating about 30% overestimation of the leakage inductance.

#### V. CONCLUSIONS

This paper introduces a novel analytical expression to accurately calculate the leakage inductance of high power density magnetic components in which reliable loss and parasitic evaluation is the key for designing the transformer, as well as for keeping the switching losses within acceptable ranges. Hence, using the energy method, a frequency-dependent expression yielding higher accuracy in comparison with the previous analytical methods has been developed. Moreover, the derived

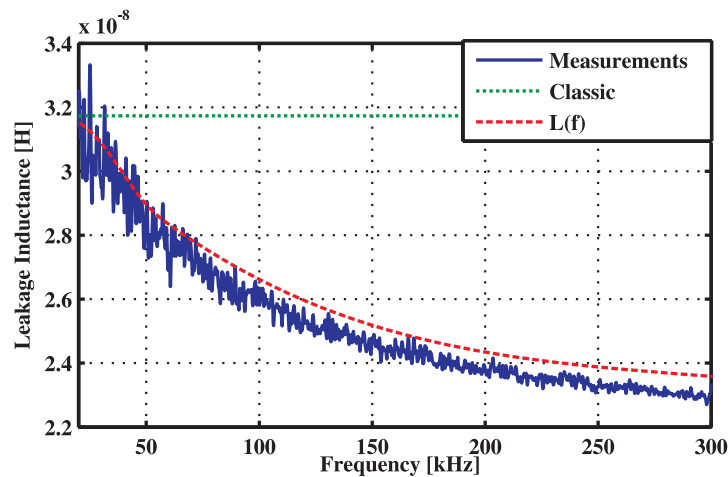


Fig. 6: Comparison between the measured leakage inductance and the calculated values by the frequency dependent and classical expressions.

expression has a wide range of applicability taking into account multilayer configuration, a wide range of penetration ratio and frequencies. In addition, it accounts for the position of the windings in the transformer window with its respective dimensions. The high accuracy together with its wide range of applications makes the final expression a useful tool that designers and researchers can easily implement within any optimization loops with almost no accuracy compromise.

#### ACKNOWLEDGMENT

This project has been funded by the Swedish Energy Agency. A great thank goes to them for the financial support.

#### REFERENCES

- [1] T. Kjellqvist, S. Norrga, and S. Ostlund, "Design considerations for a medium frequency transformer in a line side power conversion system," in *Power Electronics Specialists Conference, 2004. PESC 04. 2004 IEEE 35th Annual*, vol. 1, june 2004, pp. 704 – 710 Vol.1.
- [2] D. Dujic, F. Kieferndorf, F. Canales, and U. Drofenik, "Power electronic traction transformer technology," in *Power Electronics and Motion Control Conference (IPEMC), 2012 7th International*, vol. 1, june 2012, pp. 636 –642.
- [3] M. A. Bahmani, E. Agheb, T. Thiringer, H. K. HÅ, idalen, and Y. Serdyuk, "Core loss behavior in high frequency high power transformers—i: Effect of core topology," *Journal of Renewable and Sustainable Energy*, vol. 4, no. 3, p. 033112, 2012.
- [4] M. Wasekura, C.-M. Wang, Y. Maeda, and R. Lorenz, "A transient core loss calculation algorithm for soft magnetic composite material," in *Energy Conversion Congress and Exposition (ECCE), 2013 IEEE*, 2013, pp. 3719–3725.
- [5] M. Bahmani, T. Thiringer, and H. Ortega, "An accurate pseudoempirical model of winding loss calculation in hf foil and round conductors in switchmode magnetics," *Power Electronics, IEEE Transactions on*, vol. 29, no. 8, pp. 4231–4246, Aug 2014.
- [6] Z. Ouyang, O. Thomsen, and M. A. E. Andersen, "The analysis and comparison of leakage inductance in different winding arrangements for planar transformer," in *Power Electronics and Drive Systems, 2009. PEDS 2009. International Conference on*, Nov 2009, pp. 1143–1148.
- [7] F. de Leon, S. Purushothaman, and L. Qaseer, "Leakage inductance design of toroidal transformers by sector winding," *Power Electronics, IEEE Transactions on*, vol. 29, no. 1, pp. 473–480, Jan 2014.
- [8] J. Li, C. Hu, and X. Pang, "Analysis of the leakage inductance of planar transformer," in *Electronic Measurement Instruments, 2009. ICEMI '09. 9th International Conference on*, Aug 2009, pp. 1–273–1–276.
- [9] J. Collins, "An accurate method for modeling transformer winding capacitances," in *Industrial Electronics Society, 1990. IECON '90., 16th Annual Conference of IEEE*, Nov 1990, pp. 1094–1099 vol.2.
- [10] F. Blache, J.-P. Keradec, and B. Cogitore, "Stray capacitances of two winding transformers: equivalent circuit, measurements, calculation and lowering," in *Industry Applications Society Annual Meeting, 1994., Conference Record of the 1994 IEEE*, Oct 1994, pp. 1211–1217 vol.2.
- [11] R. T. Naayagi, A. Forsyth, and R. Shuttleworth, "High-power bidirectional dc-dc converter for aerospace applications," *Power Electronics, IEEE Transactions on*, vol. 27, no. 11, pp. 4366–4379, 2012.
- [12] A. Alonso, J. Sebastian, D. Lamar, M. Hernando, and A. Vazquez, "An overall study of a dual active bridge for bidirectional dc/dc conversion," in *Energy Conversion Congress and Exposition (ECCE), 2010 IEEE*, Sept 2010, pp. 1129–1135.
- [13] R. De Doncker, D. Divan, and M. Kheraluwala, "A three-phase soft-switched high-power-density dc/dc converter for high-power applications," *Industry Applications, IEEE Transactions on*, vol. 27, no. 1, pp. 63–73, 1991.
- [14] A. Pernia, F. Nuno, E. Corominas, and J. Lopera, "Resonant converter controlled by variable leakage inductance in the transformer (lic)," in *Power Electronics and Applications, 1993., Fifth European Conference on*, Sep 1993, pp. 124–129 vol.3.
- [15] B. Nathan and V. Ramanarayanan, "Analysis, simulation and design of series resonant converter for high voltage applications," in *Industrial Technology 2000. Proceedings of IEEE International Conference on*, vol. 1, Jan 2000, pp. 688–693 vol.2.
- [16] P. Dowell, "Effects of eddy currents in transformer windings," *Electrical Engineers, Proceedings of the Institution of*, vol. 113, no. 8, pp. 1387 –1394, august 1966.
- [17] W. Colonel and K. T. McLyman, *Transformer and Inductor Design Handbook, Fourth Edition*. CRC Press, 2011.
- [18] W. F. Flanagan, *Handbook of Transformer Design and Applications, Second Edition*. McGraw-Hill, 1992.